Published in final edited form as:
J Neurochem. 2011 March ; 116(6): 1097–1111. doi:10.1111/j.1471-4159.2010.07165.x.

Oxidative stress induced oligomerization inhibits the activity of the non-receptor tyrosine phosphatase $STEP_{61}$

Ishani Deb[*], **Ranjana Poddar**[*], and **Surojit Paul**[§,¶,*]

[*]University of New Mexico Health Sciences Center, Department of Neurology, 1 University of New Mexico, Albuquerque, NM – 87131

[§]University of New Mexico Health Sciences Center, Department of Neurosciences, 1 University of New Mexico, Albuquerque, NM – 87131

Abstract

The neuron-specific tyrosine phosphatase STEP (STriatal Enriched Phosphatase) is emerging as an important mediator of glutamatergic transmission in the brain. STEP is also thought to be involved in the etiology of neurodegenerative disorders that are linked to oxidative stress such as Alzheimer's disease and cerebral ischemia. However the mechanism by which oxidative stress can modulate STEP activity is still unclear. In the present study we have investigated whether dimerization may play a role in regulating the activity of STEP. Our findings show that $STEP_{61}$, the membrane associated isoform, can undergo homodimerization under basal conditions in neurons. Dimerization of $STEP_{61}$ involves intermolecular disulfide bond formation between two cysteine residues (Cys 65 and Cys 76 respectively) present in the hydrophobic region at the N-terminus specific to $STEP_{61}$. Oxidative stress-induced by hydrogen peroxide leads to a significant increase in the formation of dimers and higher order oligomers of $STEP_{61}$. Using two substrates, *para*-nitrophenylphosphate and ERK MAPK we further demonstrate that oligomerization leads to a significant reduction in its enzymatic activity.

Keywords

STEP; tyrosine phosphatase; dimerization; hydrogen peroxide; ERK

INTRODUCTION

Tyrosine phosphorylation plays a central role in many different cellular processes and aberrant alteration in the tyrosine phosphorylation of proteins is thought to be responsible for numerous diseases (Hunter 2009). Tyrosine phosphorylation is governed by opposing actions of two families of enzymes, the protein tyrosine kinases (PTKs) and protein tyrosine phosphatases (PTPs) (Hunter 1995). The PTP family includes more than 100 known members consisting of both receptor and non-receptor tyrosine phosphatases. Receptor tyrosine phosphatases are predominantly found at the plasma membrane and comprise a variable extracellular domain, a transmembrane region and usually two conserved C-terminal phosphatase domain (D1 and D2) of which the membrane-distal D2 domain is inactive. In contrast most non-receptor tyrosine phosphatases are cytosolic proteins containing one phosphatase domain with the exception of a few that are attached to different intracellular membranes (den Hertog 1999; Paul and Lombroso 2003; Stoker 2005b).

[¶]Corresponding Author: Surojit Paul, PhD University of New Mexico Health Sciences Center, Department of Neurology, 1, University of New Mexico, Albuquerque, NM – 87131 Tel: (505) 272-0610 Fax: (505) 272-8306 spaul@salud.unm.edu.

Pharmacological studies and analysis of the expression pattern have established roles of a number of PTPs in regulation of diverse aspects of neuronal function (Johnson and Van Vactor 2003).

The non-receptor tyrosine phosphatase STEP (STriatal Enriched Phosphatase; also known as Ptpn5) is one such PTP that is predominantly expressed in neurons of the basal ganglia, hippocampus, cortex and related structures (Boulanger et al. 1995). The STEP-family of PTPs includes both cytosolic ($STEP_{46}$) and membrane associated ($STEP_{61}$) variants that are formed by alternative splicing of a single gene (Bult et al. 1997). Immunocytochemical, biochemical and electron microscopic studies have localized $STEP_{61}$ to the endoplasmic reticulum (ER) (Bult et al. 1996) and post-synaptic densities (Oyama et al. 1995). Both $STEP_{61}$ and $STEP_{46}$ contain a highly conserved substrate-binding domain termed the kinase interacting motif or KIM domain (Pulido et al. 1998). Dopamine/D1 receptor mediated phosphorylation of a critical serine residue in the KIM domain renders STEP inactive in terms of its ability to bind to its substrate (Paul et al. 2000). In contrast, glutamate-mediated stimulation of NR2B-containing NMDA receptors leads to dephosphorylation of this residue, allowing STEP to bind to its substrates. This includes two members of the mitogen-activated protein kinase (MAPK) family, extracellular-regulated kinase (ERK1/2) and stress-activated kinase p38 MAPK (Paul et al. 2003; Xu et al. 2009; Paul and Connor 2010; Poddar et al. 2010). Through its regulation of ERK MAPK activity, STEP can interfere with memory consolidation in a Pavlovian fear-conditioning paradigm, suggesting a role in modulating synaptic plasticity (Paul et al. 2007). STEP is thought to modulate NMDA receptor-dependent long term potentiation by interfering with NMDA receptor trafficking to synaptic membranes (Pelkey et al. 2002), possibly through regulation of the upstream kinase Fyn or tyrosine dephosphorylation of NMDA receptor subunits (Nguyen et al. 2002; Snyder et al. 2005). Impairment of NMDA receptor trafficking also plays a role in the pathogenesis of Alzheimer's disease (AD) and an observed increase in $STEP_{61}$ levels in the post-mortem brains of patients suffering from AD may suggest a role of STEP in AD related dementia (Kurup et al. 2010). Additionally STEP has also been shown to regulate AMPA receptor trafficking following stimulation of group I metabotropic glutamate receptors (Zhang et al. 2008). Several studies also indicate a role of STEP in neuroprotection through its regulation of p38 MAPK activity (Xu et al. 2009; Poddar et al. 2010). Taken together the above findings suggest that STEP is emerging as an important regulator of neuronal function and viability.

The present study was undertaken to understand the mechanisms involved in the regulation of STEP's activity. A major finding of this work is that the enzymatic activity of $STEP_{61}$ is regulated by intermolecular dimerization. Using molecular and biochemical methods in cell lines and primary neuronal cultures we have identified the domain involved in dimerization of $STEP_{61}$ and further demonstrated that oxidative stress leads to increased oligomerization and loss of activity of $STEP_{61}$.

MATERIALS AND METHODS

Materials and reagents

Pregnant female Sprague-Dawley rats (16-day gestation) and adult male rats (250–300 g) were from Harlan Laboratories (Livermore, CA, USA). Approval for animal experiments was given by the University of New Mexico, Health Sciences Center, Institutional Animal Care and Use Committee. Cos-7, HEK 293, Hela and Neuro 2A cells were obtained from American Type Culture Collection (Manassas, VA). Details of all antibodies, recombinant proteins and reagents are provided in Appendix S1.

DNA constructs

Full-length $STEP_{61}$ and $STEP_{46}$ cDNAs were constructed in mammalian expression vector pcDNA3.1 encoding C-terminal V5 and His tags or myc and His tags. Deletion and point mutants of $STEP_{61}$ were obtained by polymerase chain reaction (PCR) based site-directed mutagenesis using Pfu Turbo DNA polymerase (Stratagene, La Jolla, CA, USA) according to manufacturer's protocol. All mutants were verified by nucleotide sequencing.

Cell culture and stimulation

Primary neuronal cultures were obtained from 16–17 day old rat embryos as described previously (Paul et al. 2003). For studies using cell lines we routinely used Cos-7, Hela, HEK 293 and Neuro 2A cells. A brief summary of cell culture methods as well as mutant cDNAs and stimulants used for the study are described in Appendix S1.

Detection of dimers and oligomers using co-immunoprecipitation and non-reducing SDS-PAGE

For immunoprecipitation experiments cells transfected with both V5-tagged and myc-tagged STEP constructs were lysed and then processed for immunoprecipitation of STEP with anti-V5 or anti-myc antibody as described in Appendix S1. To detect the dimers and higher oligomers of STEP, cell lysates obtained from HEK 293 cells transfected with $STEP_{61}$ cDNA or neuronal cells were processed for SDS-PAGE and immunoblot analysis under reducing and non-reducing conditions as described in Appendix S1. Densitometric analysis of immunoblots was performed using Image J Software (NIH, Bethesda, MD, USA). Statistical comparison was carried out using one-way analysis of variance (ANOVA, Bonferroni's multiple comparison test) and differences were considered significant when $p < 0.05$.

DTT treatment

Treatment of cells with dithiothreitol (DTT) was performed as described previously (Walchli et al. 2005). A brief summary of the method has been described in Appendix S1.

Phosphatase activity assay

Phosphatase activity of STEP was determined using both *para*-nitrophenylphosphate (pNPP) assay and tyrosine dephosphorylation of phosphorylated-ERK2. A detail description of the method has been provided in Appendix S1.

RESULTS

Intermolecular interaction of $STEP_{61}$ in intact cells

To determine whether the membrane bound isoform of STEP ($STEP_{61}$), can form intermolecular interaction in intact cells V5- and myc-tagged $STEP_{61}$ cDNAs were co-expressed in HEK 293 cells. $STEP_{61}$-V5 was immunoprecipitated using an anti-V5 antibody and co-immunoprecipitation of $STEP_{61}$-myc was determined by immunoblotting with an anti-myc antibody. Figure 1A (upper panel, lane 2) shows that $STEP_{61}$-myc readily co-immunoprecipitates with $STEP_{61}$-V5. The specificity of this interaction was confirmed by the absence of any $STEP_{61}$-myc band in V5-pull downs from cells transfected only with $STEP_{61}$-V5 or $STEP_{61}$-myc (Fig. 1A, upper panel, lanes 3 and 4). Re-probing the blot with anti-V5 antibody (Fig. 1A, middle panel) and immunoblot analysis of the input lysates with anti-myc antibody (Fig. 1A, lower panel) ensured equal expression of both $STEP_{61}$-V5 and $STEP_{61}$-myc in transfected cells. Similar results were obtained when $STEP_{61}$-myc was immunoprecipitated using anti-myc antibody and co-immunoprecipitation of $STEP_{61}$-V5 was determined using anti-V5 antibody (Fig. 1B). These results indicate that $STEP_{61}$ may

form dimers in living cells. To ensure that intermolecular interaction of $STEP_{61}$ is not a cell-specific event, the above experiment was repeated in Hela, Cos-7 and Neuro 2A cell lines. As observed in the HEK 293 cells, $STEP_{61}$-myc readily associates with $STEP_{61}$-V5 in Hela, Cos-7 and Neuro 2A cells (Fig. S1). To determine whether the cytosolic variant of STEP ($STEP_{46}$), can also interact with each other in intact cells HEK 293 cells were transfected with V5- and myc-tagged $STEP_{46}$ or $STEP_{61}$. The results indicate that $STEP_{46}$ failed to form intermolecular interaction in intact cells (Fig. 1C). To further determine if $STEP_{61}$ can interact with $STEP_{46}$, HEK 293 cells were co-transfected with myc-tagged $STEP_{61}$ and V5-tagged $STEP_{46}$. The findings indicate that $STEP_{61}$ fails to pull down $STEP_{46}$ (Fig. 1D).

Involvement of N-terminal cysteine residues in dimerization of $STEP_{61}$

We next generated a panel of both V5- and myc-tagged deletion mutants to determine the role of different domains in the intermolecular interaction of $STEP_{61}$. A schematic diagram of these deletion constructs are shown in Figure 2A. $STEP_{61}$ differs from the cytosolic variant ($STEP_{46}$) by the presence of a unique 172 amino acid containing region at the N-terminus that contains two hydrophobic domains (HD1 and HD2) and two polyproline rich domains (PP1 and PP2). Both $STEP_{61}$ and $STEP_{46}$ isoforms contain the KIM domain and the phosphatase domain (PTP). Deletion of the PTP domain that is known to be involved in the dimerization of receptor tyrosine phosphatases (Tonks 2006) failed to block intermolecular interaction of $STEP_{61}$ (Fig. 2B). Deletion of the KIM domain or the polyproline rich regions (PP1 and PP2) that are involved in protein-protein interaction (Pawson 1995; Pulido et al. 1998) also had no effect on $STEP_{61}$ interaction (Fig. 2C). However N-terminal deletion of the first polyproline rich region (PP1) and the adjacent hydrophobic domain (HD1) in $STEP_{61}$ (amino acids 2–83) resulted in a near total loss of the intermolecular interaction (Fig. 2D). Deletion of amino acids 84 –171 containing the second polyproline rich region (PP2) and the adjacent hydrophobic domain (HD2) resulted in loss of expression of $STEP_{61}$ (data not shown).

The N-terminal domain of $STEP_{61}$ that is involved in intermolecular interaction (aa 2–83) contains four cysteine residues (Fig. 3A). We next examined whether intermolecular disulfide bond formation involving these cysteine residues may lead to dimerization of $STEP_{61}$. In initial experiments, HEK 293 cells co-expressing V5- and myc-tagged $STEP_{61}$ were exposed to DTT (50 mM) for 30 min to disrupt endogenous disulfide bridges between cysteine residues. The cells were then lysed in the presence of iodoacetamide (IODA), which irreversibly binds to free-sulfhydryl groups thereby preventing any disulfide bond formation during lysis (Lee et al. 1998;van der Wijk et al. 2004;Walchli et al. 2005). This was followed by immunoprecipitation of V5-tagged $STEP_{61}$. Co-immunoprecipitation of myc-tagged $STEP_{61}$ was determined by immunoblot analysis with anti-myc antibody. A significant reduction in intermolecular interaction of $STEP_{61}$ (20.8% ± 6.4 of control, $p < 0.0001$) was observed in the presence of DTT and IODA (Fig. 3B) suggesting that one or more cysteine residues within the deleted region was essential for the formation of stable $STEP_{61}$ dimers. To directly test the role of these cysteine residues in the dimerization of $STEP_{61}$ we mutated Cys 2, Cys 3, Cys 65 or Cys 76 in $STEP_{61}$. Both V5- and myc-tagged variants of these single mutants were co-expressed in HEK 293 cells followed by coimmunoprecipitation studies to test their ability to form dimers. Mutation of Cys 2 or 3 to Ser in $STEP_{61}$ had no effect on intermolecular interaction of $STEP_{61}$ (Fig. 3C, left panel). A similar pattern was observed when both Cys 2 and 3 were mutated to Ser (Fig. 3C, right panel). In contrast, mutation of Cys 65 or Cys 76 to Ser resulted in significant reduction in intermolecular interaction of $STEP_{61}$ (Fig. 3D, left panel; 38.4% ± 3.4 and 35.2% ± 4.8 of control, $p < 0.0001$). Consistent with this, mutation of both Cys 65 and Cys 76 to Ser almost completely abolished intermolecular interaction of $STEP_{61}$ (3D, right panel; 13.5% ± 3.6 of control, $p < 0.0001$). Taken together these results suggest that intermolecular disulfide

linkages between Cys 65 and Cys 76 respectively are involved in the dimerization of $STEP_{61}$.

Hydrogen peroxide induces oligomerization of $STEP_{61}$

Oxidative stress induced by a variety of pathological conditions produces reactive oxygen species (ROS) that have been shown to modulate intermolecular interaction between receptor tyrosine phosphatases (Tonks 2006). To determine whether H_2O_2 induced oxidative stress can alter the basal level of dimerization of $STEP_{61}$, HEK 293 cells expressing both V5- and myc-tagged $STEP_{61}$ were treated with different concentrations of H_2O_2 (0, 1, 10 and 100 mM) for 5 min. $STEP_{61}$-V5 was immunoprecipitated using anti-V5 antibody and immune complexes were processed for immunoblotting with anti-myc antibody. Exposure to H_2O_2 resulted in a dose-dependent increase in co-immunoprecipitation of myc-tagged $STEP_{61}$ and a significant increase in complex formation was observed with 10 mM and higher concentrations of H_2O_2 (Fig. 4A). It is well established that dimers and higher order associations (oligomers) generated due to intermolecular disulfide bond formation leads to an upward shift in electrophoretic mobility of proteins on SDS-PAGE when analyzed under non-reducing conditions. To determine whether dimerization of $STEP_{61}$ can also lead to an upward shift in mobility under non-reducing conditions, total lysates were obtained from HEK 293 cells expressing $STEP_{61}$-V5 and treated with varying concentrations of H_2O_2. These were then subjected to SDS-PAGE in the absence of β-mercaptoethanol (non-reducing conditions) followed by immunoblot analysis with anti-V5 antibody. H_2O_2 treatment resulted in a concentration-dependent migration of $STEP_{61}$ to positions that correspond to double (between 100 –150 kDa) and even higher molecular weights (between 150 – 250 kDa and above 250 kDa) compared to the $STEP_{61}$ monomer (Fig. 4B, upper panel) suggesting the formation of dimers and higher order associations (oligomers). Formation of such oligomers under non-reducing conditions in response to oxidative stress has also been reported in earlier studies involving receptor tyrosine phosphatases (van der Wijk et al. 2004; Walchli et al. 2005; Lee et al. 2007). The increasing amount of $STEP_{61}$ oligomer formation also coincided with a corresponding decrease in its monomeric form under non-reducing conditions (Fig. 4B, upper panel). Immunoblot analysis of the same samples under reducing conditions (in the presence of β-mercaptoethanol) did not show any of the higher order bands of $STEP_{61}$ that were observed under non-reducing conditions (Fig. 4B, middle panel) and the monomeric form remained unchanged. A comparison of Figure 4A and 4B (right panel) shows that the dose-dependent increase in oligomer formation detected under non-reducing conditions was similar in profile to the observed increase in dimer formation detected by co-immunoprecipitation of differentially tagged $STEP_{61}$ cDNAs.

To examine the temporal profile of $STEP_{61}$ oligomerization, cells co-transfected with V5- and myc-tagged $STEP_{61}$ were treated with 10 mM H_2O_2 for varying times (0 –10 min). This was followed by immunoprecipitation of V5-tagged $STEP_{61}$ and immunoblot analysis with anti-myc antibody. The results showed a time-dependent increase in co-immunoprecipitation of myc-tagged $STEP_{61}$ along with V5-tagged $STEP_{61}$ (Fig. 4C). A time dependent increase in oligomer formation was also observed when total lysates obtained from cells expressing $STEP_{61}$-V5 and treated with H_2O_2 were analyzed under non-reducing conditions (Fig. 4D). The formation of oligomers under non-reducing conditions and dimers in the co-immunoprecipitation experiments showed similar temporal profiles (compare Fig. 4C and D, right panel). Taken together the above study suggests that H_2O_2 induced oxidative stress leads to a significant increase in oligomerization of $STEP_{61}$. To determine whether oligomerization of $STEP_{61}$ is a reversible phenomenon in subsequent experiments HEK 293 cells over-expressing $STEP_{61}$-V5 were treated with different concentrations of H_2O_2 (1 and 10 mM) for 5 min. The cells were then returned to its original medium and maintained for

varying times (0–30 min). As shown earlier, treatment with H_2O_2 led to increased oligomerization of $STEP_{61}$ under non-reducing conditions (Fig. S2A and B, lane 2). However removal of H_2O_2 resulted in a significant decrease in the oligomeric forms at both 15 and 30 min (Fig. S2A and B, lanes 3 and 4), suggesting that this reaction is reversible.

To examine the consequences of mutating both Cys 65 and Cys 76 ($STEP_{61}$ C65S/C76S) on intermolecular interaction, V5- and myc-tagged $STEP_{61}$ WT or $STEP_{61}$ C65S/C76S mutants were co-expressed in HEK 293 cells. Co-immunoprecipitation experiments showed that mutation of the cysteine residues severely reduced interaction between V5 and myc-tagged $STEP_{61}$ (Fig. 5, lane 3; 16.6% ± 4.3 of WT control). With subsequent exposure to H_2O_2 (10 mM, 5 min) levels of dimerization of the mutant form increased (Fig. 5, lane 4; 39.4% ± 10.2), but was still significantly lower than that of $STEP_{61}$ WT treated with H_2O_2 (Fig. 5, lane 2; 231.8% ± 10.1 of WT control). The consequence of this mutation was substantial enough to reduce the dimerization level of the mutant form in the presence of H_2O_2 even below that observed in $STEP_{61}$ WT under basal condition (Fig. 5, compare lanes 1 and 4; 39.4% ± 10.2 for mutant as compared to 100% for WT). Although the final levels were low the extent of dimerization of the mutant form in the presence of H_2O_2 was significantly higher than its corresponding control (Fig. 5, compare lanes 3 and 4; 39.4% ± 10.2 in the presence of H_2O_2 as compared to 16.6% ± 4.3 in the absence of H_2O_2). This raises the possibility that H_2O_2 induced increase in oligomerization of $STEP_{61}$ is independent of Cys 65 and Cys 76 and may involve other cysteine residues.

Oligomerization is accompanied by a decrease in PTPase activity of $STEP_{61}$

We next investigated whether H_2O_2 induced oligomerization had any effect on the phosphatase activity of $STEP_{61}$WT and its mutant form ($STEP_{61}$ C65S/C76S). HEK 293 cells expressing V5-and myc-tagged $STEP_{61}$ or its mutant form were treated with 10 mM H_2O_2 for 5 min or left untreated. Tyrosine phosphatase activity of immunoprecipitated $STEP_{61}$ was measured using pNPP as a substrate and the values were normalized for the amount of STEP immunoprecipitated. Under basal condition a four fold increase in phosphatase activity of the mutant form was observed, as compared to $STEP_{61}$WT (Fig. 6A), supporting a role of the two cysteine residues in the basal dimerization and decrease in phosphatase activity of $STEP_{61}$WT. Addition of H_2O_2 led to significant reduction in phosphatase activity of $STEP_{61}$WT (Fig. 6A, 3.77% ± 4.3) as compared to the untreated control (25% ± 4.3). Exposure to H_2O_2 also decreased the phosphatase activity of the mutant form significantly (>Fig. 6A, 19.77% ± 4.3, 5-fold) as compared to the untreated control (100%) and was slightly below that observed in $STEP_{61}$ WT under basal condition (25% ± 4.3). However, the activity of the mutant form was still five fold higher than that of $STEP_{61}$WT treated with H_2O_2 (19.77% ± 4.3 for mutant versus 3.77% ± 4.3 for WT), indicating that the basal dimerization of $STEP_{61}$ involving Cys 65 and Cys75 may facilitate the increased loss of its activity.

To obtain a more physiologically relevant measure of phosphatase activity we next examined the ability of dimerized $STEP_{61}$ to dephosphorylate one of its biological substrates, ERK2 (Paul et al. 2003). HEK 293 cells co-expressing $STEP_{61}$-V5 and $STEP_{61}$-myc were treated with H_2O_2 (10 mM) for 5 min. $STEP_{61}$ immunoprecipitated with anti-V5 antibody from H_2O_2 treated and untreated cells were incubated with phosphorylated ERK2 fusion protein (T^PEY^P-ERK2) for 30 min and then analyzed by immunoblotting using an anti-TEY^P-ERK1/2 antibody. Our results show that $STEP_{61}$ immunoprecipitated from H_2O_2 treated cells was less effective in dephosphorylating ERK2 as compared to that immunoprecipitated from untreated cells (Fig. 6B, upper panel and corresponding bar graph). Re-probing the blot with anti-myc antibody confirmed the presence of increased dimer forms of $STEP_{61}$ in H_2O_2 treated cells (Fig. 6B, third panel) suggesting that dimerization leads to a strong decrease in intrinsic phosphatase activity of $STEP_{61}$.

Hydrogen peroxide induced oligomerization and decrease in activity of $STEP_{46}$

To examine the effect of H_2O_2 on oligomerization of $STEP_{46}$, if any, V5- and myc-tagged $STEP_{46}$ (WT) co-expressed in HEK 293 cells were exposed to H_2O_2 (10 mM) for 5 min. Coimunoprecipitation experiments shows that $STEP_{46}$-myc readily co-immunoprecipitates with $STEP_{46}$-V5 in the presence of H_2O_2 (Fig. S3A, lane 2). The appearance of both dimeric (between 75–100 kDa) and oligomeric (between 100–250 kDa and above) forms of $STEP_{46}$ was also evident when cell lysates obtained from HEK 293 cells transfected with V5-tagged $STEP_{46}$ were analyzed under non-reducing condition (Fig. S3B, lane 2). Measurement of the phosphatase activity of $STEP_{46}$ further showed a substantial decrease in the phosphatase activity in the presence of H_2O_2 (Fig. S3C; 40.3% ± 2.4 of control). Taken together with the findings in Figure 6A it appears that oligomerization of both $STEP_{61}$ and $STEP_{46}$ in the presence of H_2O_2 may involve additional sites that may be responsible, at least in part, for the reduction in their phosphatase activity.

Oligomerization of $STEP_{61}$ in neurons

We next examined if endogenous $STEP_{61}$, expressed in the brain and neuronal cultures, can form dimers and higher order oligomers in the same way as observed in cells over-expressing $STEP_{61}$. In initial studies lysates obtained from cortex and hippocampus of adult rat brain as well as that obtained from neuronal cultures (12–14 days *in vitro*) were analyzed under non-reducing conditions. The findings show that under basal condition varying levels of $STEP_{61}$ dimer (between 100 ~ 150 kDa) are present in the cortex, hippocampus and cultured neurons (Fig. 7) with the maximum level being found in the cortex (~ 50%). Under reducing conditions the higher order band of $STEP_{61}$ was absent and the monomeric form remained unchanged (Fig. 7). Analysis of lysates from striatal homogenates that expresses both $STEP_{61}$ and $STEP_{46}$, under non-reducing condition also demonstrated the presence of the dimeric form, although at low levels (data not shown). Treatment of neuronal cultures with different concentrations of H_2O_2 (0.1 – 10 mM) for 5 min resulted in a dose-dependent increase in oligomer formation (Fig. 8A, upper panel and corresponding bar graph) and a corresponding decrease in the monomeric form of $STEP_{61}$ (Fig. 8A, upper panel), which is consistent with our earlier findings in cells transfected with $STEP_{61}$ constructs (Fig. 4B). Under reducing conditions the monomeric form remained unchanged (Figure 10A, middle panel). Exposure to 10 mM H_2O_2 for varying times (1 – 10 min) also resulted in a time-dependent increase in the oligomer forms of $STEP_{61}$ (Fig. 8B, upper panel and corresponding bar graph) and a parallel decrease in the monomeric form (Fig. 8B, upper panel) under non-reducing conditions. As expected, the monomeric form remained unchanged under reducing conditions (Fig. 8B, middle panel). Since STEP is expressed endogenously in neurons we further examined the effect of different concentrations of H_2O_2 (1 and 10mM) on phosphorylation of ERK, a physiological substrate of STEP. Immunoblot analysis of neuronal lysates with anti- TEY^P-ERK1/2 antibody showed a similar increase in tyrosine phosphorylation of ERK2 from 2.5 min onwards (Fig. 8C) at both the doses studied. To determine if dimerization of endogenous STEP may well be responsible for the phosphorylation of ERK we synthesized a TAT-STEP peptide that is transducible in neurons and can bind constitutively to ERK. Earlier studies have shown that this peptide can attenuate the phosphorylation of its substrates, ERK and p38 MAP kinase in intact cells (Paul et al. 2007;Xu et al. 2009;Poddar et al. 2010). Pre-incubation with this peptide blocked H_2O_2 mediated phosphorylation of ERK (Fig. 8D). Taken together these results suggest oxidative stress induced dimerization and subsequent inactivation of $STEP_{61}$ may play a role in sustained activation of ERK2 in neurons.

DISCUSSION

The current study shows that $STEP_{61}$, the membrane-associated variant of STEP, can form dimers under basal conditions both in neurons and in transfected cells. Basal dimerization of $STEP_{61}$ involves intermolecular disulfide bond formation involving Cys 65 and Cys 76 present in a hydrophobic domain specific to $STEP_{61}$ and results in substantial loss of phosphatase activity. Oxidative stress caused by H_2O_2 resulted in the formation of higher order oligomers of $STEP_{61}$ and further decrease in phosphatase activity. Although $STEP_{46}$ does not dimerize under basal condition exposure to H_2O_2 leads to formation of oligomers and moderate loss of activity. These results further our understanding of the regulation and function of $STEP_{61}$ and $STEP_{46}$ by oxidative stress.

The concept of dimerization or oligomerization as a regulatory mechanism of $STEP_{61}$ was tested using multiple approaches that have been used in earlier studies (Blanchetot et al. 2002; Xu and Weiss 2002; Toledano-Katchalski et al. 2003; van der Wijk et al. 2004; Walchli et al. 2005; Noordman et al. 2008). The co-immunoprecipitation studies provide strong evidence for physical proximity of the two differentially tagged molecules of $STEP_{61}$ and may involve direct intermolecular interaction or sharing of a binding partner. The studies with DTT indicate that such interaction involves the formation of intermolecular disulfide bridges. The two cysteine residues mediating this interaction include Cys 65 and Cys 76 and are present in the unique N-terminal domain of $STEP_{61}$. Single mutation of either one of the cysteine residues led to considerable decrease in intermolecular interaction, whereas double mutation of both the residues completely abolished the interaction. Such graded response following single or double mutation provides strong support for the involvement of intermolecular disulfide linkages in dimer formation of $STEP_{61}$. Consistent with these findings additional studies using immunoblot analysis under non-reducing conditions shows the presence of a band that corresponds to approximately double the molecular weight of monomeric $STEP_{61}$ in hippocampus, cortex, neurons and cells transfected with $STEP_{61}$. Oxidative stress induced by H_2O_2 also led to the appearance of dimeric forms in $STEP_{46}$ and higher order bands in both $STEP_{61}$ and $STEP_{46}$ suggestive of oligomerization of the protein.

Dimerization is a well-known regulatory mechanism for transmembrane proteins that includes receptor tyrosine phosphatases (Lemmon and Schlessinger 1994; den Hertog et al. 2008). However dimerization of native receptor tyrosine phosphatases has been difficult to observe and has mostly been reported using chimeric proteins, and chemical cross-linkers (Desai et al. 1993; Jiang et al. 1999; Walchli et al. 2005; Lee et al. 2007). In contrast, intermolecular association of the non-receptor tyrosine phosphatase, $STEP_{61}$, is readily detectable under basal conditions suggesting that homodimerization is an inherent property of $STEP_{61}$. Multiple domains are known to be involved in dimerization of receptor tyrosine phosphatases and include the extracellular domain (Jiang et al. 2000; Xu and Weiss 2002; Walchli et al. 2005), transmembrane domain (Chin et al. 2005; Noordman et al. 2008) and the membrane distal phosphatase domain, D2 (Blanchetot et al. 2002; Toledano-Katchalski et al. 2003; van der Wijk et al. 2004). Several lines of evidence indicate that ligand binding to the extracellular domains of receptor tyrosine phosphatases induces receptor dimerization that in turn may regulate the catalytic phosphatase activity (Meng et al. 2000; Fukada et al. 2006). However, to date, very few biologically relevant ligands have been identified for receptor tyrosine phosphatases and this has limited our understanding of how extracellular interactions regulate dimerization and activity of the cytoplasmic phosphatase domain (Stoker 2005a). In this context, dimerization of $STEP_{61}$ is unique since it lacks extracellular, transmembrane and D2 domains. To our knowledge this is the first study that demonstrates homodimerization of a non-receptor tyrosine phosphatase involving a domain that is not conserved among PTPs. Further investigations are necessary to determine whether other

non-receptor tyrosine phosphatases can form dimers, involving such nonconserved domains, and evaluate their possible effects on intracellular signaling pathways.

Under basal conditions wild-type $STEP_{61}$ is partially dimerized, while the mutant form ($STEP_{61}$ C65S/C76S) fails to form significant amounts of dimer. Exposure to H_2O_2 led to a ~2.5-fold increase in the dimer form of wild-type $STEP_{61}$ within 5 min. It is possible that in the pre-stimulation situation a dynamic equilibrium exists between the monomeric and dimeric forms where the monomeric state is preferred due to the reducing environment in the cytoplasm. Oxidative stress such as the one caused by H_2O_2 provides a more oxidizing environment in the cytoplasm leading to stabilization of disulfide bridges at Cys 65 and Cys 76. H_2O_2 may also induce the formation of disulfide bonds between other redox-sensitive cysteine residues. Earlier studies have reported that intracellular ROS generation can readily oxidize cysteine residues in several tyrosine phosphatases favoring formation of sulfenic acid. Catalytic site cysteine residues are most susceptible because of their low pK_a (Groen et al. 2005; Tonks 2005; Paulsen and Carroll 2009). Biochemical and structural studies have shown that such reversibly inactivated catalytic cysteine residues can be further stabilized by intermolecular disulfide bond formation with the catalytic cysteine of a related monomer (van der Wijk et al. 2004). Such reversible oxidation may contribute, at least in part, to the increased dimerization of $STEP_{61}$ WT in an oxidizing environment. It may as well explain the increase in dimerization of the mutant form of $STEP_{61}$ ($STEP_{61}$ C65S/C76S) and the formation of dimers in $STEP_{46}$ in the presence of H_2O_2. In the current study we also show that that a substantial portion of $STEP_{61}$ maintains the monomeric form even after treatment with high concentration of H_2O_2, both in HEK 293 cells and in neurons. Although the reason for this is not known it is possible that there are two pools of $STEP_{61}$ that are differentially regulated in response to stimuli. Consistent with this interpretation earlier studies have reported that $STEP_{61}$ is localized in the post-synaptic density as well as the endoplasmic reticulum and might differ in their response to H_2O_2.

The loss of phosphatase activity of PTPs in response to various oxidants, including H_2O_2, has been attributed, at least in part, to the oxidation of the catalytic site cysteine residue (Finkel 1998). Several studies have also shown that besides oxidation of catalytic cysteine residue additional events, including dimerization, are responsible for inactivation of PTPs in response to oxidative stress (Blanchetot et al. 2002; Xu and Weiss 2002; Toledano-Katchalski et al. 2003; van der Wijk et al. 2004; Walchli et al. 2005; Noordman et al. 2008). It has also been proposed that oxidation of the catalytic cysteine residue may facilitate confirmational changes to stabilize the dimeric forms of PTPs (Groen et al. 2008). Thus it appears that activity of PTPs is regulated through concomitant action of both oxidation and dimerization. Consistent with this hypothesis our data shows that intermolecular disulfide bridge formation involving two cysteine residues plays a role in decreased activity of $STEP_{61}$ under basal condition. Exposure to H_2O_2 results in increased oligomerization and loss of activity of both $STEP_{61}$WT and its mutant as well as that of $STEP_{46}$WT. However, the loss of activity of $STEP_{61}$WT is five fold higher than the mutant form. Also a comparison of the PTP activity of $STEP_{61}$WT and $STEP_{46}$WT in the presence of H_2O_2 shows that the decrease in activity of $STEP_{61}$ (6.6 fold) is significantly higher than that of $STEP_{46}$ (2.5 fold). This increased loss of activity of $STEP_{61}$ cannot be explained by the oxidation of catalytic cysteine residue alone. It is possible that the existing disulfide bridges, in $STEP_{61}$, involving Cys 65 and 76 stabilize additional intermolecular interaction. As such the loss of activity, in the presence of H_2O_2, may partly result from oligomerization and may partly be attributed to the oxidation of the active site cysteine residue. Identification of the additional site(s) that are involved in oligomerization of $STEP_{61}$ (WT and mutant form) and $STEP_{46}$ and their precise contribution in the loss of activity of STEP in response to H_2O_2 is an important topic for future study.

H_2O_2 is one of the most abundant forms of ROS that is relatively more stable *in vivo* and membrane permeable (Adam-Vizi 2005). Although the precise intracellular level of H_2O_2 under pathologic conditions is not known, it is thought to be present between micromolar and millimolar ranges (Beckman and Ames 1998; Benzing et al. 1999; Shen et al. 2008). Neurons appear to be particularly susceptible to oxidative stress and brief exposures to varying concentrations of H_2O_2 (0.1 – 10 mM) have been shown to result in a profound and delayed neuronal cell death (Desagher et al. 1996; Avshalumov and Rice 2002; Fonfria et al. 2005; Wu et al. 2007). Both exogenous treatment and endogenous production of H_2O_2 has been shown to inhibit protein tyrosine phosphatases (Finkel 1998; Lee and Esselman 2002) suggesting that oxidative stress-induced neurotoxicity may be mediated through tyrosine-phosphorylation dependent signaling pathways. In this context our findings that the activity of the neuron-specific tyrosine phosphatases, $STEP_{61}$ and $STEP_{46}$, are inhibited by H_2O_2 supports the notion that inactivation of STEP may facilitate neuronal injury by promoting increased tyrosine phosphorylation of its physiological substrates that include both ERK and p38 MAPKs.

A growing number of studies have established a detrimental role of ERK MAPK during oxidative neuronal injury. For example sustained activation of ERK MAPK following exposure to H_2O_2 has been shown to induce neuronal cell death (Luo et al. 2007; Numakawa et al. 2007; Chen et al. 2009; Tuerxun et al. 2010). Sustained activation of ERK MAPK by prolonged exposure to glutamate (5 mM), which causes oxidative stress, also leads to caspase dependent neuronal cell death (Stanciu et al. 2000). In these studies inhibition of ERK MAPK has also been shown to protect neurons against oxidative stress induced death. These findings suggest a probable impairment of negative feedback regulators in response to oxidative stress that normally function to limit the duration of ERK-mediated signaling. Consistent with this hypothesis, earlier studies have shown that ERK MAPK is a substrate of STEP and active STEP may promote neuronal survival by limiting the duration of ERK MAP kinase activation (Paul et al. 2003). The inability of dimerized $STEP_{61}$ to dephosphorylate ERK described in the present study suggests that inactivation of STEP may be a missing link between ROS generation and chronic activation of ERK in neurons which expresses STEP endogenously. Several studies have also indicated a role of p38 MAP kinase, another substrate of STEP, in oxidative stress-induced neurodegeneration. p38 activation through NO produced by neuronal nitric oxide synthase following glutamate stimulated NMDA receptor and PSD95-nNOS interaction is involved in neuronal cell death (Kawasaki et al. 1997; Cao et al. 2005). Its activation has also been identified in neurons exposed to 6-hydroxydopamine and 1-methyl-4-phenyl-1,2,3,6-tetrahydropyridine (MPTP), neurotoxins that triggers ROS production, and is implicated in the mechanism of cell death (Du et al. 2001; Choi et al. 2004). Thus it appears that both and ERK and p38 MAP kinase can potentially mediate the harmful events underlying oxidative stress-induced neuronal injury. Since STEP is also a target of oxidative stress, taken together the above findings suggest that inactivation of STEP through oligomerization could play a role in the initiation of neuronal degeneration by promoting chronic activation of ERK and p38 MAPK that eventually leads to activation of pro-apoptotic pathways.

In conclusion, our findings provides evidence that dimerization plays a role in regulating the activity of $STEP_{61}$ under basal condition. H_2O_2 induced oxidative stress leads to increase in oligomerization of STEP in a dose-dependent manner resulting in reduced catalytic activity. We also observed that $STEP_{46}$ that do not form dimers under basal conditions could undergo oligomerization resulting in subsequent loss of activity upon treatment with H_2O_2. Based on these findings subsequent studies will assess the effect of oligomerization of $STEP_{61}$ and $STEP_{46}$ in neurodegenerative disorders related to oxidative stress.

Supplementary Material

Refer to Web version on PubMed Central for supplementary material.

Acknowledgments

This work was supported by the National Institute of Health grant NS059962 (Paul, S). We would like to thank Dr. William Shuttleworth, University of New Mexico, for his helpful comments.

Abbreviations

STEP	striatal-enriched phosphatase
PTP	protein tyrosine phosphatase
ERK	extracellular regulated kinase
MAPK	mitogen-activated protein kinase
pNPP	*para*-nitrophenylphosphate
IODA	iodoacetamide
DTT	dithiothreitol
SDS	sodium dodecyl sulfate

REFERENCE

Adam-Vizi V. Production of reactive oxygen species in brain mitochondria: contribution by electron transport chain and non-electron transport chain sources. Antioxidants & redox signaling. 2005; 7:1140–1149. [PubMed: 16115017]

Avshalumov MV, Rice ME. NMDA receptor activation mediates hydrogen peroxide-induced pathophysiology in rat hippocampal slices. Journal of neurophysiology. 2002; 87:2896–2903. [PubMed: 12037193]

Beckman KB, Ames BN. The free radical theory of aging matures. Physiological reviews. 1998; 78:547–581. [PubMed: 9562038]

Benzing WC, Wujek JR, Ward EK, Shaffer D, Ashe KH, Younkin SG, Brunden KR. Evidence for glial-mediated inflammation in aged APP(SW) transgenic mice. Neurobiology of aging. 1999; 20:581–589. [PubMed: 10674423]

Blanchetot C, Tertoolen LG, den Hertog J. Regulation of receptor protein-tyrosine phosphatase alpha by oxidative stress. The EMBO journal. 2002; 21:493–503. [PubMed: 11847098]

Boulanger LM, Lombroso PJ, Raghunathan A, During MJ, Wahle P, Naegele JR. Cellular and molecular characterization of a brain-enriched protein tyrosine phosphatase. J Neurosci. 1995; 15:1532–1544. [PubMed: 7869116]

Bult A, Zhao F, Dirkx R Jr. Raghunathan A, Solimena M, Lombroso PJ. STEP: a family of brain-enriched PTPs. Alternative splicing produces transmembrane, cytosolic and truncated isoforms. Eur J Cell Biol. 1997; 72:337–344. [PubMed: 9127733]

Bult A, Zhao F, Dirkx R Jr. Sharma E, Lukacsi E, Solimena M, Naegele JR, Lombroso PJ. STEP61: a member of a family of brain-enriched PTPs is localized to the endoplasmic reticulum. J Neurosci. 1996; 16:7821–7831. [PubMed: 8987810]

Cao J, Viholainen JI, Dart C, Warwick HK, Leyland ML, Courtney MJ. The PSD95-nNOS interface: a target for inhibition of excitotoxic p38 stress-activated protein kinase activation and cell death. The Journal of cell biology. 2005; 168:117–126. [PubMed: 15631993]

Chen L, Liu L, Yin J, Luo Y, Huang S. Hydrogen peroxide-induced neuronal apoptosis is associated with inhibition of protein phosphatase 2A and 5, leading to activation of MAPK pathway. The international journal of biochemistry & cell biology. 2009; 41:1284–1295.

Chin CN, Sachs JN, Engelman DM. Transmembrane homodimerization of receptor-like protein tyrosine phosphatases. FEBS letters. 2005; 579:3855–3858. [PubMed: 15978577]

Choi WS, Eom DS, Han BS, Kim WK, Han BH, Choi EJ, Oh TH, Markelonis GJ, Cho JW, Oh YJ. Phosphorylation of p38 MAPK induced by oxidative stress is linked to activation of both caspase-8- and -9-mediated apoptotic pathways in dopaminergic neurons. The Journal of biological chemistry. 2004; 279:20451–20460. [PubMed: 14993216]

den Hertog J. Protein-tyrosine phosphatases in development. Mech Dev. 1999; 85:3–14. [PubMed: 10415342]

den Hertog J, Ostman A, Bohmer FD. Protein tyrosine phosphatases: regulatory mechanisms. The FEBS journal. 2008; 275:831–847. [PubMed: 18298791]

Desagher S, Glowinski J, Premont J. Astrocytes protect neurons from hydrogen peroxide toxicity. J Neurosci. 1996; 16:2553–2562. [PubMed: 8786431]

Desai DM, Sap J, Schlessinger J, Weiss A. Ligand-mediated negative regulation of a chimeric transmembrane receptor tyrosine phosphatase. Cell. 1993; 73:541–554. [PubMed: 8490965]

Du Y, Ma Z, Lin S, Dodel RC, Gao F, Bales KR, Triarhou LC, Chernet E, Perry KW, Nelson DL, Luecke S, Phebus LA, Bymaster FP, Paul SM. Minocycline prevents nigrostriatal dopaminergic neurodegeneration in the MPTP model of Parkinson's disease. Proceedings of the National Academy of Sciences of the United States of America. 2001; 98:14669–14674. [PubMed: 11724929]

Finkel T. Oxygen radicals and signaling. Current opinion in cell biology. 1998; 10:248–253. [PubMed: 9561849]

Fonfria E, Marshall IC, Boyfield I, Skaper SD, Hughes JP, Owen DE, Zhang W, Miller BA, Benham CD, McNulty S. Amyloid beta-peptide(1–42) and hydrogen peroxide-induced toxicity are mediated by TRPM2 in rat primary striatal cultures. Journal of neurochemistry. 2005; 95:715–723. [PubMed: 16104849]

Fukada M, Fujikawa A, Chow JP, Ikematsu S, Sakuma S, Noda M. Protein tyrosine phosphatase receptor type Z is inactivated by ligand-induced oligomerization. FEBS letters. 2006; 580:4051–4056. [PubMed: 16814777]

Groen A, Overvoorde J, van der Wijk T, den Hertog J. Redox regulation of dimerization of the receptor protein-tyrosine phosphatases RPTPalpha, LAR, RPTPmu and CD45. The FEBS journal. 2008; 275:2597–2604. [PubMed: 18422654]

Groen A, Lemeer S, van der Wijk T, Overvoorde J, Heck AJ, Ostman A, Barford D, Slijper M, den Hertog J. Differential oxidation of protein-tyrosine phosphatases. The Journal of biological chemistry. 2005; 280:10298–10304. [PubMed: 15623519]

Hunter T. Protein kinases and phosphatases: the yin and yang of protein phosphorylation and signaling. Cell. 1995; 80:225–236. [PubMed: 7834742]

Hunter T. Tyrosine phosphorylation: thirty years and counting. Current opinion in cell biology. 2009; 21:140–146. [PubMed: 19269802]

Jiang G, den Hertog J, Hunter T. Receptor-like protein tyrosine phosphatase alpha homodimerizes on the cell surface. Mol Cell Biol. 2000; 20:5917–5929. [PubMed: 10913175]

Jiang G, den Hertog J, Su J, Noel J, Sap J, Hunter T. Dimerization inhibits the activity of receptor-like protein-tyrosine phosphatase-alpha. Nature. 1999; 401:606–610. [PubMed: 10524630]

Johnson KG, Van Vactor D. Receptor protein tyrosine phosphatases in nervous system development. Physiological reviews. 2003; 83:1–24. [PubMed: 12506125]

Kawasaki H, Morooka T, Shimohama S, Kimura J, Hirano T, Gotoh Y, Nishida E. Activation and involvement of p38 mitogen-activated protein kinase in glutamate-induced apoptosis in rat cerebellar granule cells. The Journal of biological chemistry. 1997; 272:18518–18521. [PubMed: 9228012]

Kurup P, Zhang Y, Xu J, Venkitaramani DV, Haroutunian V, Greengard P, Nairn AC, Lombroso PJ. Abeta-mediated NMDA receptor endocytosis in Alzheimer's disease involves ubiquitination of the tyrosine phosphatase STEP61. J Neurosci. 2010; 30:5948–5957. [PubMed: 20427654]

Lee K, Esselman WJ. Inhibition of PTPs by H(2)O(2) regulates the activation of distinct MAPK pathways. Free radical biology & medicine. 2002; 33:1121–1132. [PubMed: 12374624]

Lee S, Faux C, Nixon J, Alete D, Chilton J, Hawadle M, Stoker AW. Dimerization of protein tyrosine phosphatase sigma governs both ligand binding and isoform specificity. Mol Cell Biol. 2007; 27:1795–1808. [PubMed: 17178832]

Lee SR, Kwon KS, Kim SR, Rhee SG. Reversible inactivation of protein-tyrosine phosphatase 1B in A431 cells stimulated with epidermal growth factor. The Journal of biological chemistry. 1998; 273:15366–15372. [PubMed: 9624118]

Lemmon MA, Schlessinger J. Regulation of signal transduction and signal diversity by receptor oligomerization. Trends Biochem Sci. 1994; 19:459–463. [PubMed: 7855887]

Luo J, Kintner DB, Shull GE, Sun D. ERK1/2-p90RSK-mediated phosphorylation of Na+/H+ exchanger isoform 1. A role in ischemic neuronal death. The Journal of biological chemistry. 2007; 282:28274–28284. [PubMed: 17664275]

Meng K, Rodriguez-Pena A, Dimitrov T, Chen W, Yamin M, Noda M, Deuel TF. Pleiotrophin signals increased tyrosine phosphorylation of beta beta-catenin through inactivation of the intrinsic catalytic activity of the receptor-type protein tyrosine phosphatase beta/zeta. Proceedings of the National Academy of Sciences of the United States of America. 2000; 97:2603–2608. [PubMed: 10706604]

Nguyen TH, Liu J, Lombroso PJ. Striatal enriched phosphatase 61 dephosphorylates Fyn at phosphotyrosine 420. The Journal of biological chemistry. 2002; 277:24274–24279. [PubMed: 11983687]

Noordman YE, Augustus ED, Schepens JT, Chirivi RG, Rios P, Pulido R, Hendriks WJ. Multimerisation of receptor-type protein tyrosine phosphatases PTPBR7 and PTPSL attenuates enzymatic activity. Biochim Biophys Acta. 2008; 1783:275–286. [PubMed: 18068678]

Numakawa Y, Matsumoto T, Yokomaku D, Taguchi T, Niki E, Hatanaka H, Kunugi H, Numakawa T. 17beta-estradiol protects cortical neurons against oxidative stress-induced cell death through reduction in the activity of mitogen-activated protein kinase and in the accumulation of intracellular calcium. Endocrinology. 2007; 148:627–637. [PubMed: 17082253]

Oyama T, Goto S, Nishi T, Sato K, Yamada K, Yoshikawa M, Ushio Y. Immunocytochemical localization of the striatal enriched protein tyrosine phosphatase in the rat striatum: a light and electron microscopic study with a complementary DNA-generated polyclonal antibody. Neuroscience. 1995; 69:869–880. [PubMed: 8596655]

Paul S, Lombroso PJ. Receptor and nonreceptor protein tyrosine phosphatases in the nervous system. Cell Mol Life Sci. 2003; 60:2465–2482. [PubMed: 14625689]

Paul S, Connor JA. NR2B-NMDA receptor mediated increases in intracellular Ca(2+) concentration regulate the tyrosine phosphatase, STEP, and ERK MAP kinase signaling. Journal of neurochemistry. 2010; 114:1107. [PubMed: 20524968]

Paul S, Nairn AC, Wang P, Lombroso PJ. NMDA-mediated activation of the tyrosine phosphatase STEP regulates the duration of ERK signaling. Nat Neurosci. 2003; 6:34–42. [PubMed: 12483215]

Paul S, Snyder GL, Yokakura H, Picciotto MR, Nairn AC, Lombroso PJ. The Dopamine/D1 receptor mediates the phosphorylation and inactivation of the protein tyrosine phosphatase STEP via a PKA-dependent pathway. J Neurosci. 2000; 20:5630–5638. [PubMed: 10908600]

Paul S, Olausson P, Venkitaramani DV, Ruchkina I, Moran TD, Tronson N, Mills E, Hakim S, Salter MW, Taylor JR, Lombroso PJ. The striatal-enriched protein tyrosine phosphatase gates long-term potentiation and fear memory in the lateral amygdala. Biol Psychiatry. 2007; 61:1049–1061. [PubMed: 17081505]

Paulsen CE, Carroll KS. Orchestrating redox signaling networks through regulatory cysteine switches. ACS Chem Biol. 2009; 5:47–62. [PubMed: 19957967]

Pawson T. Protein modules and signalling networks. Nature. 1995; 373:573–580. [PubMed: 7531822]

Pelkey KA, Askalan R, Paul S, Kalia LV, Nguyen TH, Pitcher GM, Salter MW, Lombroso PJ. Tyrosine phosphatase STEP is a tonic brake on induction of long-term potentiation. Neuron. 2002; 34:127–138. [PubMed: 11931747]

Poddar R, Deb I, Mukherjee S, Paul S. NR2B-NMDA receptor mediated modulation of the tyrosine phosphatase STEP regulates glutamate induced neuronal cell death. Journal of neurochemistry. 2010 In Press.

Pulido R, Zuniga A, Ullrich A. PTP-SL and STEP protein tyrosine phosphatases regulate the activation of the extracellular signal-regulated kinases ERK1 and ERK2 by association through a kinase interaction motif. The EMBO journal. 1998; 17:7337–7350. [PubMed: 9857190]

Shen C, Chen Y, Liu H, Zhang K, Zhang T, Lin A, Jing N. Hydrogen peroxide promotes Abeta production through JNK-dependent activation of gamma-secretase. The Journal of biological chemistry. 2008; 283:17721–17730. [PubMed: 18436531]

Snyder EM, Nong Y, Almeida CG, Paul S, Moran T, Choi EY, Nairn AC, Salter MW, Lombroso PJ, Gouras GK, Greengard P. Regulation of NMDA receptor trafficking by amyloid-beta. Nat Neurosci. 2005; 8:1051–1058. [PubMed: 16025111]

Stanciu M, Wang Y, Kentor R, Burke N, Watkins S, Kress G, Reynolds I, Klann E, Angiolieri MR, Johnson JW, DeFranco DB. Persistent activation of ERK contributes to glutamate-induced oxidative toxicity in a neuronal cell line and primary cortical neuron cultures. The Journal of biological chemistry. 2000; 275:12200–12206. [PubMed: 10766856]

Stoker A. Methods for identifying extracellular ligands of RPTPs. Methods. 2005a; 35:80–89. [PubMed: 15588989]

Stoker AW. Protein tyrosine phosphatases and signalling. J Endocrinol. 2005b; 185:19–33. [PubMed: 15817824]

Toledano-Katchalski H, Tiran Z, Sines T, Shani G, Granot-Attas S, den Hertog J, Elson A. Dimerization in vivo and inhibition of the nonreceptor form of protein tyrosine phosphatase epsilon. Mol Cell Biol. 2003; 23:5460–5471. [PubMed: 12861030]

Tonks NK. Redox redux: revisiting PTPs and the control of cell signaling. Cell. 2005; 121:667–670. [PubMed: 15935753]

Tonks NK. Protein tyrosine phosphatases: from genes, to function, to disease. Nature reviews. 2006; 7:833–846.

Tuerxun T, Numakawa T, Adachi N, Kumamaru E, Kitazawa H, Kudo M, Kunugi H. SA4503, a sigma-1 receptor agonist, prevents cultured cortical neurons from oxidative stress-induced cell death via suppression of MAPK pathway activation and glutamate receptor expression. Neuroscience letters. 2010; 469:303–308. [PubMed: 20025928]

van der Wijk T, Overvoorde J, den Hertog J. H2O2-induced intermolecular disulfide bond formation between receptor protein-tyrosine phosphatases. The Journal of biological chemistry. 2004; 279:44355–44361. [PubMed: 15294898]

Walchli S, Espanel X, Hooft van Huijsduijnen R. Sap-1/PTPRH activity is regulated by reversible dimerization. Biochem Biophys Res Commun. 2005; 331:497–502. [PubMed: 15850787]

Wu YN, Martella G, Johnson SW. Rotenone enhances N-methyl-D-aspartate currents by activating a tyrosine kinase in rat dopamine neurons. Neuroreport. 2007; 18:1813–1816. [PubMed: 18090317]

Xu J, Kurup P, Zhang Y, Goebel-Goody SM, Wu PH, Hawasli AH, Baum ML, Bibb JA, Lombroso PJ. Extrasynaptic NMDA receptors couple preferentially to excitotoxicity via calpain-mediated cleavage of STEP. J Neurosci. 2009; 29:9330–9343. [PubMed: 19625523]

Xu Z, Weiss A. Negative regulation of CD45 by differential homodimerization of the alternatively spliced isoforms. Nature immunology. 2002; 3:764–771. [PubMed: 12134145]

Zhang Y, Venkitaramani DV, Gladding CM, Zhang Y, Kurup P, Molnar E, Collingridge GL, Lombroso PJ. The tyrosine phosphatase STEP mediates AMPA receptor endocytosis after metabotropic glutamate receptor stimulation. J Neurosci. 2008; 28:10561–10566. [PubMed: 18923032]

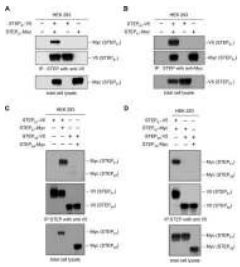

Figure 1.

$STEP_{61}$ forms homodimers in intact cells. V5- and myc-tagged $STEP_{61}$ or $STEP_{46}$ were co-expressed in HEK 293 cells. STEP was immunoprecipitated using anti-V5 (A, C, D) or anti-myc (B) antibodies followed by immunoblot analysis. Blots were probed with anti-myc (A, C and D - upper panel; B - middle panel) and anti-V5 (A, C and D - middle panel; B - upper panel) antibodies. Expression of myc-tagged $STEP_{61}$ (A, C and D), $STEP_{46}$ (C and D) and V5-tagged $STEP_{61}$ (B) in the total lysate was monitored in the lower panel.

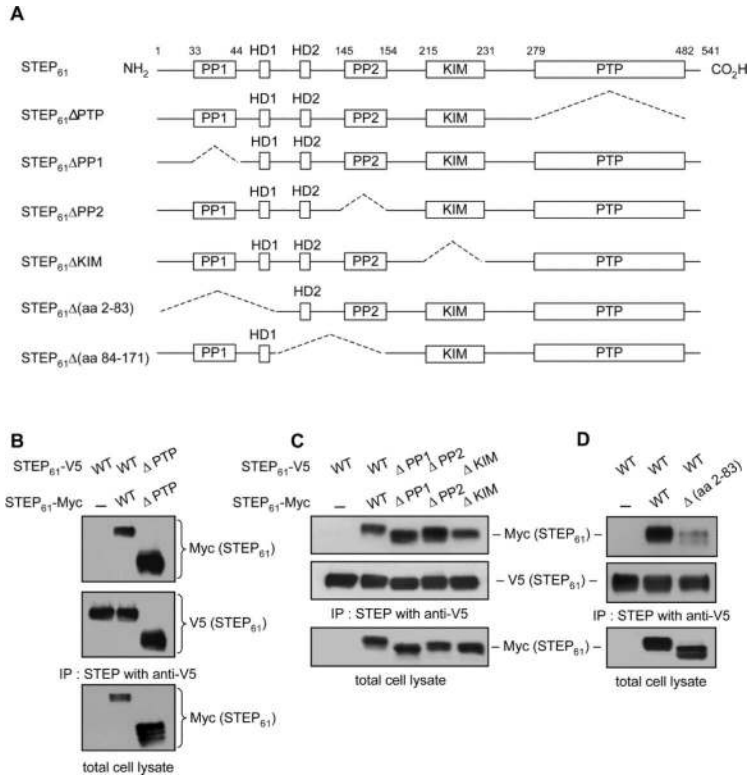

Figure 2.

Role of N-terminal region of $STEP_{61}$ in homodimer formation. (A) Schematic representation of the deletion mutants of $STEP_{61}$ used in the co-immunoprecipitation experiments depicted in B, C and D. The domains deleted were tyrosine phosphatase domain (ΔPTP), polyproline rich region 1 (ΔPP1), polyproline rich region 2 (ΔPP2), Kinase interacting motif (ΔKIM), N-terminal amino acids 2 – 83 Δ(aa 2–83) and 84–171 Δ(aa 84–171) . (B, C, and D) V5- and myc-tagged $STEP_{61}$ deletion mutants were expressed in HEK 293 cells. Following immunoprecipitation of V5-tagged $STEP_{61}$ co-immunoprecipitation of myc-tagged $STEP_{61}$was determined using anti-myc antibody (upper panel). Blots were re-probed with anti-V5 antibody (middle panel). Equal expression of myc-tagged $STEP_{61}$ in total lysate was determined by immunoblot analysis using anti-myc antibody (lower panel).

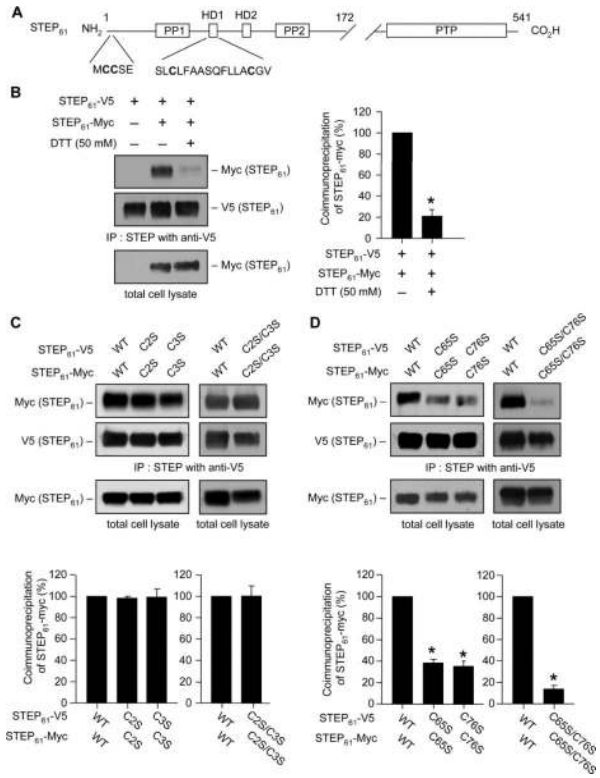

Figure 3.

Cys 65 and Cys 76 are required for intermolecular disulfide bond formation. (A) Schematic diagram of $STEP_{61}$ showing the positions of all the cysteine residues (in bold) in the N-terminal domain within aa 2–83. (B) HEK 293 cells expressing V5- and myc-tagged $STEP_{61}$ WT were treated with DTT (50 mM) for 30 min. (C, D) V5 and myc-tagged $STEP_{61}$ WT or single and double mutants of Cys 2, Cys3, Cys 65 and Cys 76 were expressed in HEK 293 cells. (B, C, D) Upon immunoprecipitation of $STEP_{61}$ with anti-V5, co-immunoprecipitation of myc-tagged $STEP_{61}$ was determined by probing the blots with anti-myc antibody (upper panel). Blots were re-probed with anti-V5 antibody (middle panel). Expression of myc-tagged $STEP_{61}$ in total lysate was determined by immunoblot analysis using anti-myc antibody (lower panel). Quantification of co-immunoprecipitated $STEP_{61}$-myc band (B, C, D - upper panel) was done by computer-assisted densitometry and Image J analysis. Values are mean ± SEM (n = 3). * Indicates significant difference from DTT untreated control (B) or WT (C, D) ($p < 0.0001$).

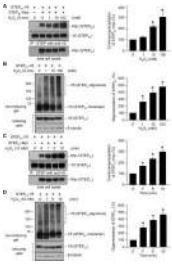

Figure 4.

H_2O_2 induced increase in dimer and higher order oligomer formation of $STEP_{61}$. HEK 293 cells transfected with V5- and myc-tagged $STEP_{61}$ (A, C) or V5-tagged $STEP_{61}$ (B and D) were stimulated (A, B) for 5 min with different concentration of H_2O_2 or (C, D) with 10 mM H_2O_2 for different time periods. (A, C) $STEP_{61}$ was immunoprecipitated with anti-V5 antibody. Blots were probed with anti-myc (upper panel) and anti-V5 (middle panel) antibodies. Expression of myc-tagged $STEP_{61}$ in total lysate was analyzed with anti-myc antibody (lower panel). (B, D) Equal amount of protein from each sample, was prepared under non-reducing conditions (without β-mercaptoethanol) to investigate oligomer formation (upper panel). Another part was loaded under reducing conditions (withβ-mercaptoethanol) to check expression levels (middle panel). Immunoblots were probed with anti-V5 antibody. Total tubulin was also analyzed to indicate equal protein loading (lower panel). Quantification of (A, C - upper panel) co-immunoprecipitated $STEP_{61}$-myc band and (B, D) oligomeric forms of $STEP_{61}$ in non-reducing gels (bands at 100 kDa and above) was done by computer-assisted densitometry and Image J analysis. Values are mean ± SEM (n = 3). * Indicates significant difference from untreated control ($p < 0.001$).

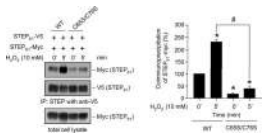

Figure 5.

Involvement of cysteine residues in H_2O_2 induced dimerization of $STEP_{61}$. WT $STEP_{61}$ or its mutant $STEP_{61}$ C65S/C76S tagged with V5- or myc-epitope co-expressed in HEK 293 cells were stimulated with 10 mM H_2O_2 for 5 min. STEP was immunoprecipitated using anti-V5 antibody. Blots were probed with anti-myc (upper panel) and anti-V5 (middle panel) antibodies. Total lysate was analyzed with anti-myc antibody (lower panel). Quantification of coimmunoprecipitated $STEP_{61}$-myc band (upper panel) was done by computer-assisted densitometry and Image J analysis. Values are mean ± SEM (n = 3). *Indicates significant difference from corresponding untreated controls ($p < 0.0001$). # Indicates significant difference from H_2O_2 treated $STEP_{61}$-V5 WT samples ($p < 0.0001$).

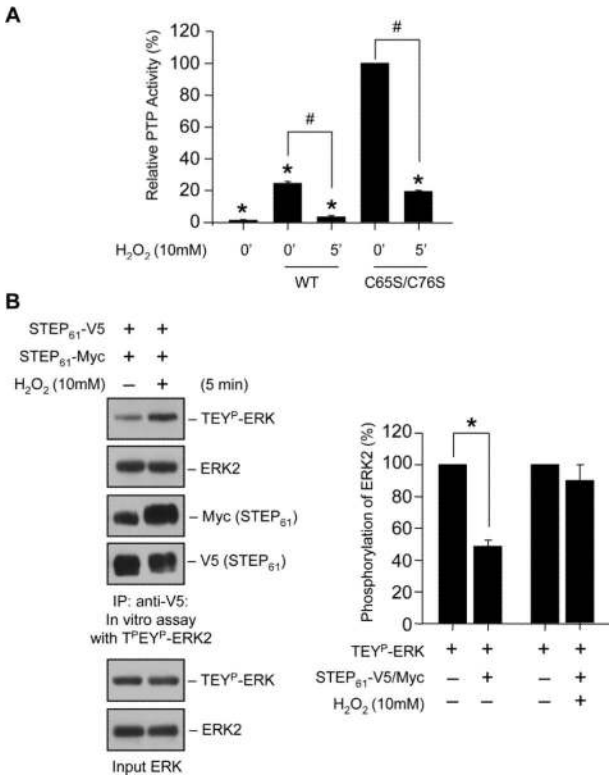

Figure 6.

H_2O_2 induced decrease in $STEP_{61}$ activity. HEK 293 cells expressing V5-and myc-tagged $STEP_{61}$ or its mutant ($STEP_{61}$ C65S/C76S) were stimulated with 10 mM H_2O_2 for the specified time periods. (A, B) $STEP_{61}$ was immunoprecipitated from H_2O_2 treated (5 min) and untreated cells using anti-V5 antibody. (A) PTP activity was assayed using pNPP as a substrate. Quantitative measurement of the formation of para-nitrophenolate is represented as mean ± SEM (n = 4). * Indicates significant difference from untreated $STEP_{61}$ mutant ($p < 0.001$). # Indicates significant difference from the untreated WT or mutant ($p < 0.001$). (B) Immunoprecipitated $STEP_{61}$ was incubated with phospho-ERK2 (T^PEY^P-ERK2) purified protein for 30 min at 30°C. Phosphorylation of ERK2 was analyzed with anti-TEY^P-ERK 1/2 (first panel) antibody. Dimerization of $STEP_{61}$ in the same samples was analyzed by re-probing the blot with anti-myc (third panel) and anti-V5 (fourth panel) antibodies. Blots were also re-probed with anti-ERK2 antibody (second panel). To determine the phosphorylation of the input phospho-ERK2, for each experiment, equal amount of the purified protein was incubated in buffer alone for 30 min at 30°C and then processed for immunoblot analysis with anti-TEY^P-ERK1/2 (fifth panel) and ERK2 (sixth panel) antibodies. Extent of phosphorylation of phospho-ERK2 in the absence and presence of $STEP_{61}$ (first and fifth panel) was determined by computer-assisted densitometry and Image J analysis. Values are mean ± SEM (n = 3). *Indicates significant difference from untreated control ($p < 0.001$).

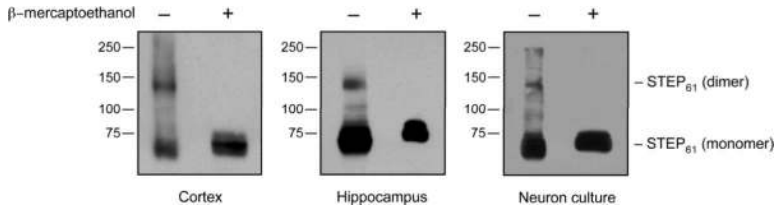

Figure 7.

Homodimerization of $STEP_{61}$ in brain and cultured neurons. Equal amount of protein obtained from hippocampal, cortical and neuronal lysates prepared under reducing (with β-mercaptoethanol) and non-reducing (without β-mercaptoethanol) conditions were processed for immunoblot analysis with anti-STEP antibody (top panel).

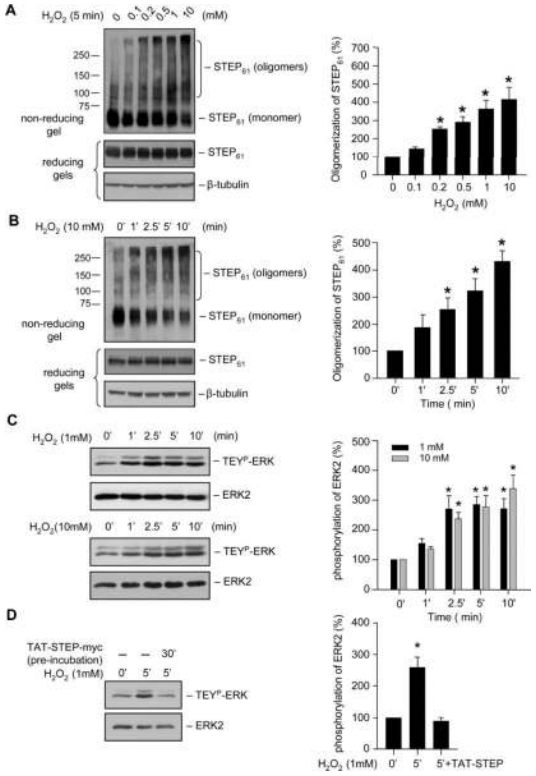

Figure 8.

Oligomerization of $STEP_{61}$ in neurons. Neuron cultures were stimulated with (A) 0 –10 mM H_2O_2 for 5 min, or (B) 10 mM H_2O_2 for 0 – 10 min, (C) 1 mM and 10 mM H_2O_2 for 0 – 10 min or (D) 1 mM H_2O_2 for 5 min in the presence or absence of the TAT-STEP peptide. (A, B) Part of the lysate was prepared under non-reducing (without β -mercaptoethanol) conditions to investigate oligomer formation (upper panel). Another part was loaded under reducing conditions (with β-mercaptoethanol) to check expression levels (middle panel). Immunoblots were probed with anti-STEP antibody. Total tubulin was also analyzed to indicate equal protein loading (lower panel). (C, D) Phosphorylation of ERK2 in total lysates was analyzed by probing the membrane with anti- TEY^P-ERK 1/2 antibody (upper panel). Blots were re-probed with anti-ERK2 antibody (lower panel). Quantification of (A, B - upper panel) oligomeric forms of $STEP_{61}$ in non-reducing gels (bands at 100 kDa and above) and (C, D - upper lane) phosphorylated ERK2 was done by computer-assisted densitometry and Image J analysis. Values are mean ± SEM (n = 3). * Indicates significant difference from untreated control ($p < 0.01$).